

# Synthesis, Characterization and Study of New Thiazole -2-amine Derivative as Corrosion Inhibitors for Mild Steel in 0.5 M H<sub>2</sub>SO<sub>4</sub> Solution

Manjunath Hegde<sup>1</sup>, S.P Nayak<sup>2\*</sup>

<sup>1</sup>Department of Chemistry, S.D.M. College, Honavar, Karnataka 581334, India

<sup>2</sup>Department of Chemistry, Mangalore University, Mangalagangothri, Karnataka 574199, India

\*Corresponding author: E-Mail: sureshnayak0104@gmail.com, Mob: 9448724552

## ABSTRACT

The derivatives of thiazole-2-amine, namely *N*-[(*E*)-(5-bromo-2-methoxyphenyl) methylidene]-4-phenyl-1,3-thiazol-2-amine (H-THS) and *N*-[(*E*)-(5-bromo-2-methoxyphenyl) methylidene]-4-(4-bromophenyl)-1,3-thiazol-2-amine (Br-THS) were synthesized and were applied as corrosion inhibitors. These compounds have been characterized by IR, <sup>1</sup>H NMR, <sup>13</sup>C NMR & LCMS spectra. The effect of thiazole compounds on the dissolution of Mild steel in 0.5M H<sub>2</sub>SO<sub>4</sub> solution was studied using weight loss and Tafel plot techniques. It was found that compounds inhibition efficiency increased with increasing concentration. The temperature influence on rate of corrosion was investigated and also some thermodynamic parameters (*E*<sub>a</sub>, Δ*H*<sup>o</sup> and Δ*S*<sup>o</sup>) were calculated. From the results we conclude that the inhibition efficiency of the inhibitors maximum at higher concentration and rate of corrosion decreases with rise in temperature. The apparent inhibitory mechanism was more supported by results obtained from polarization (Tafel plots) studies. The adsorption obeys Langmuir adsorption isotherm. The kinetic and thermodynamic parameters were calculated. The surfaces of mild steel were studied by Scanning electron microscopy (SEM) in presence and absence of inhibitors.

**KEY WORDS:** Corrosion inhibitor, Spectroscopic Studies, Adsorption, Mild Steel.

## 1. INTRODUCTION

The pipelines made by mild steel were damaged by corrosion due to carbon dioxide, acid and water present in environment is an economically and environmentally serious problem in oil and gas industries (Hong, 2001). The use of organic inhibitors was effectual method for prevent the internal parts of pipelines from corrosion (Cao, 2002; Zhao, 2004; Martinez, 2003) and it is becoming more and more popular. Thus the cost-effectiveness of the development of organic corrosion inhibitors could be reasonably crucial.

Thiazole derivatives are popular nitrogen-sulfur heterocyclic compounds that have played much attention in the past few years. It is easy to synthesize, are environmentally friendly, and exhibit wide biological activities like antitumor, cytotoxic, anti-inflammatory, antimicrobial, antioxidant, antifungal, antitubercular, anticonvulsant neuroprotective, diuretic, etc. (Kashyap, 2012). The organic compounds have inhibition efficiency is mainly depending on the structure, functional groups and chemical properties. It adsorbed on the surface of metal forms a layer. (Szyprowski, 2000). The thiazole compounds behave inhibition property due to their molecular structure.

The literature survey shows that the use of thiazole and its derivatives as inhibitors for controlling the mild steel corrosion in acidic media have been rarely reported. The aims of this work is to synthesis and study of new thiazole derivatives acts as corrosion inhibitors at different concentrations and temperatures and hence the effect on the mechanism, also calculate the activation parameter and adsorption processes in the absence and presence of thiazole-2-amine derivatives by gravimetric and electrochemical studies. Surface morphological changes of the mild steel surface were visualized by scanning electron microscopy (SEM).

## 2. MATERIALS AND METHODS

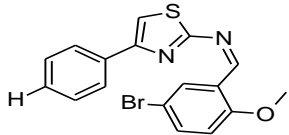
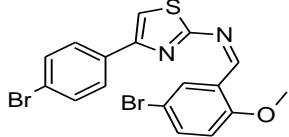
**Material Preparation:** The mild steel specimens of size 2.6 cm x 2 cm x 0.025 cm were used, it consist of C-0.051%, Mn-0.19%, Si-0.002%, P-0.018%, S-0.012%, Cr-0.019%, Mo-0.008%, Ni-0.031% and the remaining Fe, was adopted for gravimetric and electrochemical studies.

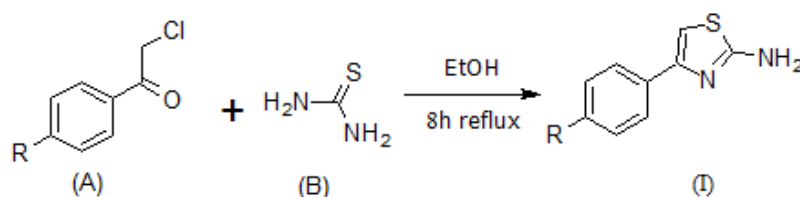
**Synthesis of Substituted 4-substituted phenyl-1,3-thiazole-2-amine derivatives(I):** Substituted thiazole-2-amine was synthesized by (1mmole) Thiourea (A) mixed with substituted (1mmole) 2-chloro-1-phenylethanone (B) in 25 ml of absolute ethanol. Heat the reaction mixture on water bath for 8 hrs with occasionally stirring. After the completion of the reaction quench the mixture in crushed ice and neutralized with 10 % aqueous KOH solution (Hong, 2009). Filter the product and washed with cold water, dried at 60°C in an oven, recrystallised from ethanol to give pure product.

**Synthesis of Substituted (5-bromo-2-methoxyphenyl)methylidene-4-substituted phenyl-1,3-thiazol-2-amine derivatives (II):** (5-bromo-2-methoxyphenyl)methylidene-4-substituted phenyl-1,3-thiazol-2-amine was prepared by 4-substituted phenyl-1,3-thiazole-2-amine (I) (1mmole) mixed with 5-bromo-2-methoxybenzaldehyde (C) (1mmole) in 20 ml of absolute ethanol and a drop of acetic acid was refluxed for 6 hours. The mixture was cooled to room temperature and poured to crushed ice. A yellow solid product was separated and collected by filtration. Recrystallize

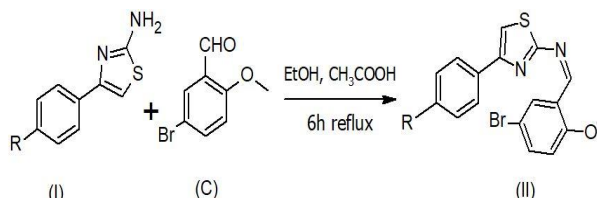
the sample using ethanol. The spectral data of H-THS and Br-THS are given in table.1.

**Table.1. Spectral data of newly synthesized compounds (II).**

Compound	IR Peak (cm <sup>-1</sup> )	<sup>1</sup> H-NMR (ppm)(CDCl <sub>3</sub> )	<sup>13</sup> C-NMR (ppm)(CDCl <sub>3</sub> )	LCMS
H-THS 	Ar-CH Str (2921), C=C Str (1588), C=N Str (1529), C-N Str(1243), C-S Str(801), CH <sub>2</sub> Str(2845).	3.81 (s, 3H, OCH <sub>3</sub> ), 6.04 (d, 1H, CH in ring), 6.20 (s, 1H, CH=N), 7.10-7.67 (m, phenyl ring), 8.36 (s, 1H CH in thiazole ring).	55.84 (OCH <sub>3</sub> ), 112 (CH in thiazole), 169.62 (C=N in ring)	m/z = 374.25 purity = 82.62 %
Br-THS 	Ar-CH Str (2914), C=C Str (1590), C=N Str (1529), C-N Str(1248), C-S Str(720), CH <sub>2</sub> Str(2852), C-Br Str(622).	3.60 (s, 3H, OCH <sub>3</sub> ), 5.9 (d, 1H, CH in ring), 6.10 (s, 1H, CH=N), 7.06-7.67 (m, phenyl ring), 8.3 (s, 1H CH in thiazole ring).	55.90 (OCH <sub>3</sub> ), 113 (CH in thiazole), 169.89 (C=N in ring)	m/z = 452.16 purity = 81.27 %



**Scheme 1: Synthesis of 4-substituted phenyl-1,3-thiazole-2-amine derivatives**



**Scheme 2: (5-bromo-2-methoxyphenyl) methylidene-4-substituted phenyl-1,3-thiazol-2-amine derivatives**

Where R = H (H-THS), R= Br (Br-THS)

**Non-Electrochemical Techniques (Weight loss method):** In weight loss measurements, with the help of glass hooks previously weighed polished mild steel coupons were immersed in a beaker containing 100 ml of 0.5M H<sub>2</sub>SO<sub>4</sub> solution in triplicates. After a period of 1 hour remove the coupons from solution, washed with distilled water, carefully dried and weighed accurately using a 5-digit balance. From change of initial weights to final weights of coupons, weight loss was calculated. Experiments were continued with different concentrations of inhibitors. The inhibition efficiency  $\eta$  (%) and surface coverage ( $\Theta$ ) of the inhibitors were calculated with the help of following equations,

$$\eta (\%) = \frac{(W_1 - W_2)}{W_1} \times 100 \quad (1)$$

$$\theta = \frac{(W_1 - W_2)}{W_1} \quad (2)$$

Where,  $W_2$  and  $W_1$  are the loss of weight of coupon in the presence and absence of the inhibitors respectively. The corrosion rate ( $C_R$ ) in mili miles penetration per year (mmpy) was calculated using following equation (Gopal, 2011),

$$C_R = \frac{87.6 \times W}{Atd} \quad (3)$$

Where  $W$  = weight loss,  $A$  = area of specimen in  $\text{cm}^2$  exposed in acidic solution,  $t$  = immersion time in hours, and  $d$  = density of mild steel ( $\text{g cm}^{-3}$ ).

**Electrochemical Studies:** Potentiodynamic polarization studies were performed using CH<sub>16</sub>O<sub>4</sub>E Electrochemical Analyzer with the help of mild steel as working electrode; saturated calomel electrode as reference electrode and platinum electrode as auxiliary electrode in 0.5M H<sub>2</sub>SO<sub>4</sub> solution at 303 K. The mild steel surface was exposed in different concentrations (from 0.25 mM to 1.00 mM) of Br-THS and H-THS inhibitors. The Tafel curves were recorded by potential range from -200 mV cathodically to +200 mV anodically at a scan rate of 0.01 V/s.

**Surface analysis:** The specimens were suspended in 100 ml of acid solution containing inhibitors over a period of 5 hours at 30°C. Wash the specimen using distilled water and dried. The surface morphology of mild steel was investigated by CARL ZEISS SIGMA MAKE scanning electron microscope.

### 3. RESULTS AND DISCUSSION

**Weight Loss Measurements:** The effect of addition of *N*-[(*E*)-(5-bromo-2-methoxyphenyl)methylidene]-4-phenyl-1,3-thiazol-2-amine and *N*-[(*E*)-(5-bromo-2-methoxyphenyl)methylidene]-4-(4-bromophenyl)-1,3-thiazol-2-amine to control the corrosion was tested on the mild steel coupon in 0.5 M H<sub>2</sub>SO<sub>4</sub> solution by weight loss measurements. From the weight loss measurements, calculate the rate of corrosion ( $C_R$ ), inhibition efficiency ( $\eta$ ) and surface coverage ( $\theta$ ) as shown in table 2. From this data it is clear that the inhibition efficiency of the inhibitors increased due to increase in concentration. Br-THS reaches maximum inhibition of 94.44 % and H-THS reaches maximum inhibition of 93.21% at  $1 \times 10^{-3}$  M. It shows that Br-THS has the more inhibition efficiency compared to H-THS. The surface coverage increases by means of preventing the metal dissolution (Ezeoke, 2012). Corrosion rate decreases from 0.25mM to 1mM concentration for each inhibitor, which reveals that increase in the inhibitor concentration decreases the corrosion rate.

**Table.2. Effect of temperature on corrosion rate and inhibition efficiency by gravimetric studies immersion at 1 h.**

Name of the Inhibitor	Temperature (K)	Concentration (mM)	Weight loss (mg)	Corrosion Rate (mmpy)	Inhibition Efficiency $E_w$ (%)	Degree of surface coverage ( $\theta$ )
Br-THS	303	blank	162	170.07		
		0.25	19	19.95	88.27	0.8827
		0.50	16	16.80	90.12	0.9012
		0.75	12	12.60	92.59	0.9259
		1.00	9	9.44	94.44	.09444
	308	blank	203	213.11		
		0.25	25	26.25	87.68	0.8768
		0.50	23	24.15	88.67	0.8867
		0.75	18	18.90	91.13	0.9113
		1.00	14	14.70	93.10	0.9310
	313	blank	267	280.29		
		0.25	48	50.39	82.02	0.8202
		0.50	45	47.24	83.14	0.8314
		0.75	36	37.80	86.52	0.8652
		1.00	31	32.54	88.39	0.8839
	318	blank	295	309.69		
		0.25	76	79.78	74.23	0.7423
		0.50	64	67.19	78.30	0.7830
		0.75	57	59.84	80.68	0.8068
		1.00	46	48.30	84.40	0.8440
	303	blank	162	170.07		
		0.25	22	23.09	86.42	0.8642
		0.50	17	17.85	89.51	0.8951
		0.75	14	14.70	91.36	0.9136
		1.00	11	11.55	93.21	0.9321
	308	blank	203	213.11		
		0.25	30	31.50	85.22	0.8522
		0.50	25	26.24	87.68	0.8768
		0.75	20	21.00	90.15	0.9015

<b>H-THS</b>		1.00	18	18.90	91.13	0.9113
	313	blank	267	280.29		
		0.25	50	52.50	81.27	0.8127
		0.50	47	49.34	82.40	0.8240
		0.75	41	43.04	84.64	0.8464
		1.00	32	33.60	88.01	0.8801
	318	blank	295	309.69		
		0.25	80	83.98	72.90	0.7290
		0.50	65	68.24	77.97	0.7797
		0.75	60	62.99	79.67	0.7967
		1.00	55	57.74	81.36	0.8136

**Effect of temperature and Kinetic study:** Effect of temperature in corrosion inhibition study plays important aspects and that can be observed by varying the temperature from 303K to 318K for different concentrations of the inhibitors. Figure.1, shows the inhibition efficiency (%) increases at higher concentration and decreases at higher temperature (Frangoza-Mar, 2012). Increase in solution temperature also increases corrosion rate expressed in figure.2.



**Figur.1. Relationship between Inhibitor concentration, Temperature and Inhibition Efficiency**  
a) Br-THS and b) H-THS

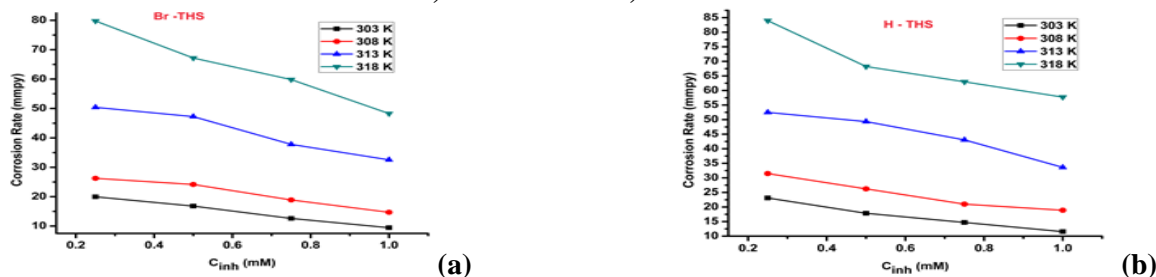


**Figure.2. Effect of Temperature on Corrosion Rate a) Br-THS and b) H-THS**

The inhibition mechanism was discussed with the help of enthalpy of activation ( $\Delta H^*$ ), activation energy ( $E_a$ ), and entropy of activation ( $\Delta S^*$ ). The activation energy ( $E_a$ ) was calculated from Arrhenius equation (Xianghong, 2009) as shown below.

$$\ln C_R = \ln A - \frac{E_a}{RT} \quad (4)$$

Where  $C_R$  is the corrosion rate,  $E_a$  is the apparent activation energy for corrosion,  $R$  is the universal gas constant,  $A$  is the Arrhenius pre-exponential factor and  $T$  is the temperature. From the figure.3, Arrhenius plot  $\ln C_R$  against  $1/T$  at different concentrations like 0.25, 0.5, 0.75 and 1.0 mM of H-THS and Br-THS inhibitors. It gives straight line with slope  $-E_a/R$  and intercept  $\ln A$ . These calculated values were represented in table.3. An activation energy ( $E_a$ ) value from Table 3 reveals that it increases from 0.25 mM to 1mM concentration of inhibitor solutions. Energy of activation increases with increase in inhibitor concentration and decreases metal dissolution by enhancing the energy barrier for the mild steel corrosion process.

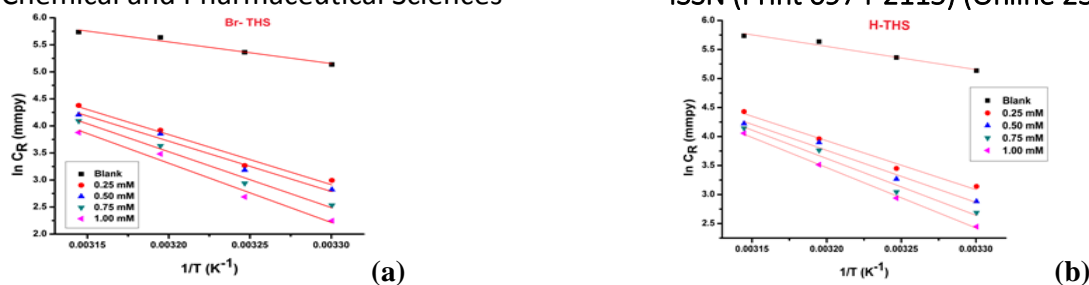


**Figure.3. Arrhenius Plot for mild steel corrosion in 0.5 M H<sub>2</sub>SO<sub>4</sub> solution: a) Br-THS and b) H-THS**

The entropy of activation ( $\Delta S^*$ ) and the activation enthalpy ( $\Delta H^*$ ) were calculated from transition state equation (Ostovari, 2009)

$$\ln \frac{C_R}{T} = \left[ \ln \frac{R}{Nh} + \frac{\Delta S^*}{R} \right] - \frac{\Delta H^*}{RT} \quad (5)$$

Where  $N$  is Avogadro's number and  $h$  is Planck's constant.

A plot of  $\ln(C_R/T)$  against  $1/T$  (Figure.4) shows the slope of  $(-\Delta H^*/R)$  and intercept  $[(\ln(R/Nh) + \Delta S^*/R)]$  from which the activation thermodynamic parameters ( $\Delta H^*$  and  $\Delta S^*$ ) were calculated and listed in table.3. From the Table 3, the  $\Delta H^*$  values in presence of Br-THS and H-THS inhibitor are 88.58 KJ/mol and 83.86 KJ/mol respectively and in pure acidic media is 28.32 KJ/mol. The positive sign indicates the enthalpy is endothermic nature of the corrosion process (Popova, 2003; Moretti, 1994). The values of  $\Delta H^*$  increase with increase of inhibitors concentration, reflects the corrosion reaction needs high energy. The  $E_a$  values of different concentration of the inhibitors are more than the  $\Delta H^*$  values indicate the corrosion process must involve a gaseous reaction, simply the hydrogen evolution reaction, associated with a decrease in the total reaction volume (Noor, 2007).

From the table.3, the  $\Delta S^*$  values for mild steel in presence of Br-THS and H-THS inhibitor are 65.68 J/mol/K and 52.16 J/mol/K respectively and without inhibitor is -108.86 J/mol/K. The above results showed that entropy of activation values are positive in the presence of inhibitors and increases with increased inhibitor concentrations and negative for the absence of inhibitor. It indicates that the activated complex in the rate-determining step shows dissociation and reaction move from reactant side to the activated complex side due to decrease in disorder (Oguzie, 2008; Dandia, 2013; Guan, 2004).

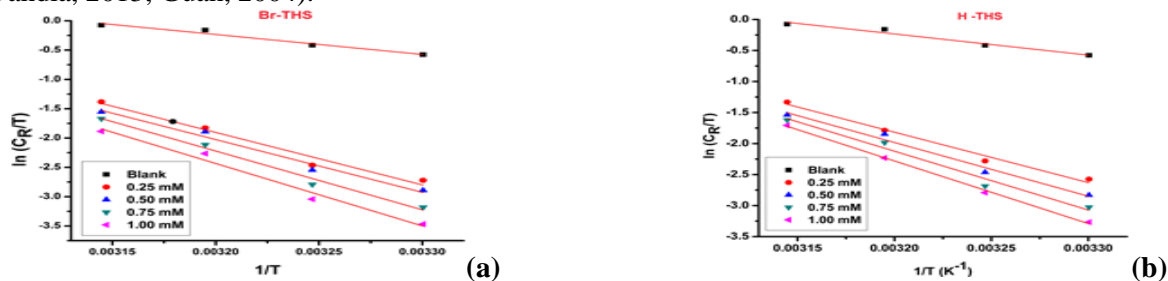


**Figure.4. Transition Plot for mild steel corrosion in 0.5 M H<sub>2</sub>SO<sub>4</sub> solution: a) Br-THS and b) H-THS**

**Adsorption Isotherm:** The interaction of adsorbed molecule on the adsorbent surface like electrode surfaces was studied by adsorption isotherm. The linear relationship between degree of surface coverage ( $\theta$ ) and inhibitor concentrations have been checked considering various isotherms like Langmuir, Temkin, and Flory-Huggins. The experimental data were verified graphically fitted to Langmuir adsorption isotherm, which is mathematically expressed as (Kumar, 2013).

$$\frac{C}{\theta} = \frac{1}{K_{ads}} + C \quad (6)$$

Where,  $K_{ads}$  is the equilibrium constant for the adsorption process.

$K_{ads}$  were calculated by plotting  $C_{inh}$  v/s  $C_{inh}/\theta$  which give linear plot values close to 1 and intercept  $1/K_{ads}$  exposed in figure.5. Calculated  $K_{ads}$  is related to free energy of adsorption ( $\Delta G^0_{ads}$ ) by (Zarrouk, 2013)

$$\Delta G^0_{ads} = -RT \ln(55.5 K_{ads}) \quad (7)$$

Where 55.5 is the concentration of water in solution expressed in mol/dm<sup>3</sup>.

The calculated  $K_{ads}$ ,  $\Delta G^0_{ads}$  values are listed in table.4. The spontaneous and non-spontaneous adsorption processes were clarified based on the value of  $\Delta G^0_{ads}$ . The results shows for both the inhibitors (H-THS and Br-THS)  $\Delta G^0_{ads}$  values are negative indicate spontaneous adsorption on mild steel surface. Generally free energy values up to -20 KJ mol<sup>-1</sup> indicates physisorption due to electrostatic interaction between charged molecules of inhibitors and metallic surfaces, while  $\Delta G^0_{ads}$  values around -40 KJ mol<sup>-1</sup> or lower, indicates chemisorptions which results in the formation of covalent bond due to sharing or transfer of electrons from the organic molecules to the metal surface (Szklarska-Smialowska, 1978; Yurt, 2006). In the present study the calculated  $\Delta G^0_{ads}$  values vary between -36.25 &

-36.95 KJ mol<sup>-1</sup> for Br-THS and -36.20 & -36.96 KJ mol<sup>-1</sup> for H-THS indicate the adsorption behavior of the inhibitors in acid solution involves both physisorption and chemisorptions (Avci, 2008; Abiola, 2004; Jeeva, 2015; Bentiss, 2005; Zou, 2014; Singh, 2012).

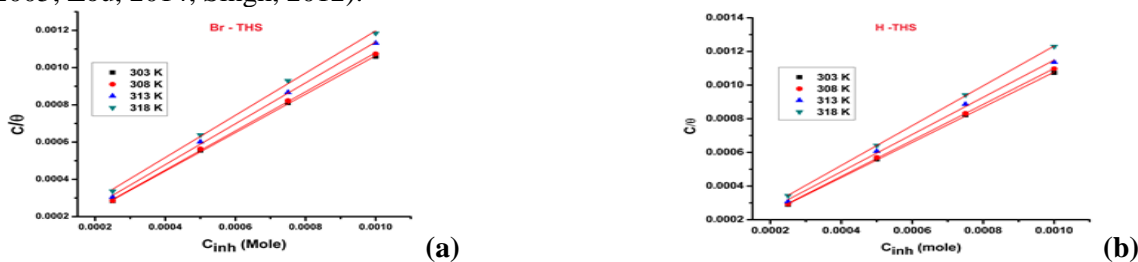


Figure.5. Langmuir Adsorption Isotherm plot: a) Br-THS and b) H-THS

Table.3. Activation parameters for Br-THS and H-THS in 0.5 M H<sub>2</sub>SO<sub>4</sub> solution

Inhibitor Name	Concentration (mM)	E <sub>a</sub> <sup>*</sup> (kJ/mol)	A (kJ/mol)	ΔH <sup>*</sup> (kJ/mol)	ΔS <sup>*</sup> (J/mol/K)
	blank	33.26	93.66 x 10 <sup>6</sup>	28.32	-108.86
Br-THS	0.25	76.97	34.25 x 10 <sup>13</sup>	74.40	24.69
	0.50	77.38	35.40 x 10 <sup>13</sup>	74.81	25.01
	0.75	85.95	78.98 x 10 <sup>14</sup>	83.34	50.78
	1.00	91.16	47.40 x 10 <sup>15</sup>	88.58	65.68
H-THS	0.25	70.14	26.94 x 10 <sup>12</sup>	67.56	3.55
	0.50	74.60	12.68 x 10 <sup>13</sup>	72.01	16.43
	0.75	81.42	15.24 x 10 <sup>14</sup>	78.84	37.10
	1.00	86.54	93.29 x 10 <sup>14</sup>	83.86	52.16

Table.4. Thermodynamic Parameters for Adsorption of Br-THS and H-THS in 0.5 M H<sub>2</sub>SO<sub>4</sub> solution on Mild Steel Surface at different temperatures

Inhibitor Name	Temperature (K)	K <sub>ads</sub> (L/mol)	ΔG <sup>0</sup> <sub>ads</sub> (kJ/mol)
Br-THS	303	3.20 x 10 <sup>4</sup>	-36.25
	308	3.33 x 10 <sup>4</sup>	-36.95
	313	2.51 x 10 <sup>4</sup>	-36.82
	318	1.57 x 10 <sup>4</sup>	-36.16
H-THS	303	1.08 x 10 <sup>4</sup>	-36.20
	308	1.12 x 10 <sup>4</sup>	-36.96
	313	1.02 x 10 <sup>4</sup>	-36.62
	318	1.01 x 10 <sup>4</sup>	-36.85

**Electrochemical Measurements (Tafel Plot Studies):** The mild steel as working electrode exposed in 100ml of 0.5M H<sub>2</sub>SO<sub>4</sub> solution at 30 °C with 0.25, 0.5, 0.75 and 1.0 mM concentrations of H-THS and Br-THS inhibitors. The Tafel curves were recorded in the potential range of -200mV to +200mV with respect to open circuit potential at a scan rate of 0.01V/s. A plot of Potential, E Vs log I, in figure.6, generates corrosion potential  $E_{corr}$ , Corrosion current  $I_{corr}$ , cathodic ( $\beta_c$ ), and anodic ( $\beta_a$ ) Tafel slope. Using the value of  $I_{corr}$ , the inhibition efficiency  $\eta_p$  (%) calculated,

$$\eta_p = \frac{I_{corr}^0 - I_{corr}}{I_{corr}^0} \times 100 \quad (8)$$

Where,  $I_{corr}$  and  $I_{corr}^0$  are the corrosion current in presence and absence of inhibitor, respectively.

All electrochemical parameters values are summarized in table.5. The results obtained showed that  $I_{corr}$  decreases with increase in inhibitor concentrations because of the active centers of mild steel surface were blocked by adsorption of inhibitor molecules. Depending on the displacement in  $E_{corr}$  value is greater than 85 mV/SCE can be considered as a cathodic or anodic type. If the displacement in  $E_{corr}$  value is less than 85 mV, indicates the corrosion inhibitor may be regarded as a mixed type (Li, 2008). The protection efficiency reaches maximum at high inhibitors concentration. The obtained inhibition efficiency values for both Br-THS and H-THS are agreeable values in comparison with values from gravimetric studies.





Figure.6. Tafel Plot for Mild steel at 303 K: (a) Br-THS and (b) H-THS

Table.5. Potentiodynamic Polarization Parameters obtained from Tafel Plot for H-THS and Br-THS at 303 K

Inhibitor	Concentration (mM)	$E_{corr}$ (mV)	$I_{corr} \times 10^{-3}$ (A)	$\beta_c$ (V/dec)	$\beta_a$ (V/dec)	$\eta_p$ (%)
	Blank	-467.5	44.0	4.581	4.695	
H-THS	0.25	-482.6	7.37	5.406	6.947	83.25
	0.50	-464.7	4.51	5.36	7.599	89.74
	0.75	-454.5	3.11	4.818	7.266	92.93
	1.00	-467.5	2.98	5.937	8.669	93.24
Br-THS	0.25	-482.0	7.13	5.492	6.971	83.80
	0.50	-464.1	4.22	5.553	7.681	90.41
	0.75	-455.8	2.92	5.051	7.328	93.35
	1.00	-467.0	2.87	6.04	8.679	93.49

**Scanning Electron Microscopy:** The SEM images of the mild steel coupon suspended in 0.5 M  $H_2SO_4$  without and with 1.00 mM of H-THS and Br-THS solution respectively are shown in figure.7. The surface of the mild steel in presence of inhibitors shows smoothness indicates corrosion rates reduced and in absence of inhibitor shows rough surface indicates corrosion rate is maximum. From the SEM analysis, inhibitors protect the mild steel surfaces.

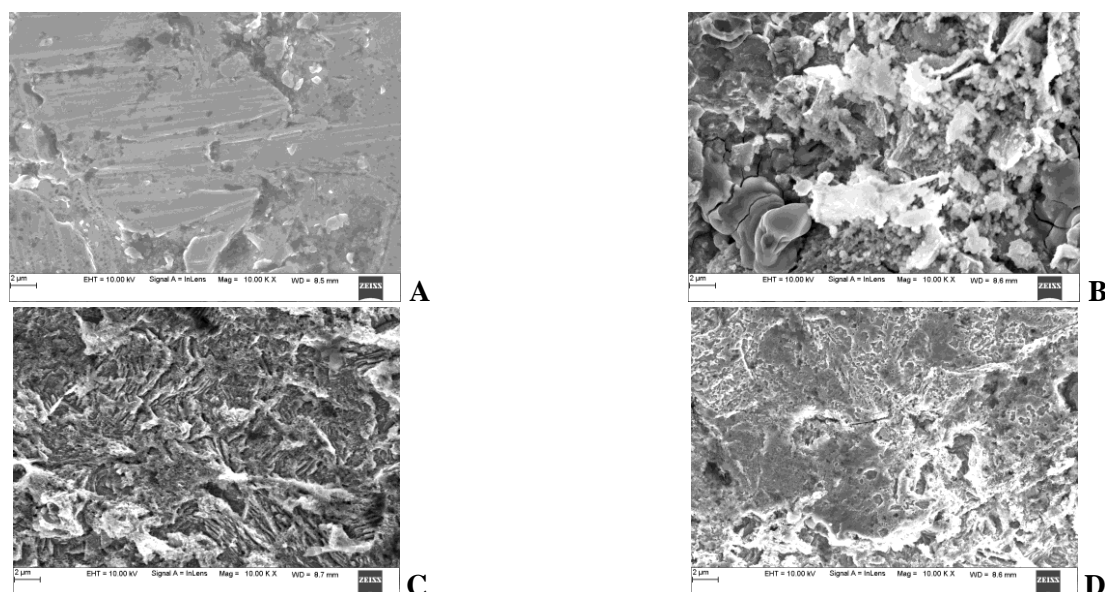


Figure.7. SEM photographs at 303 K (A) pure mild steel surface, (B) mild steel surface dipped in 0.5 M  $H_2SO_4$ , (C) mild steel surface dipped in 0.5 M  $H_2SO_4$  containing Br-THS inhibitor and (D) mild steel surface dipped in 0.5 M  $H_2SO_4$  containing H-THS inhibitor

#### 4. CONCLUSION

The Thiazole-2-amine derivatives namely *N*-[(*E*)-(5-bromo-2-methoxyphenyl)methylidene]-4-phenyl-1,3-thiazol-2-amine (H-THS) and *N*-[(*E*)-(5-bromo-2-methoxyphenyl)methylidene]-4-(4-bromophenyl)-1,3-thiazol-2-amine (Br-THS) were synthesized *via* the routes shown in step 1 and 2. The synthesized compounds were characterized by spectral analyses like IR,  $^1H$  NMR,  $^{13}C$  NMR and LCMS. The obtained data establish the structure for thiazole-2-amine. Newly synthesized compounds show excellent corrosion inhibition properties on mild steel in 0.5 M  $H_2SO_4$ . The inhibition efficiency increases with inhibitors concentration. The present study shows Br-THS compound is more inhibitory effect than H-THS compound due to substituted Br atom. From the kinetic study, corrosion rate increases with rise in solution temperature. Br-THS and H-THS adsorbed on mild steel surface and

the processes apply to Langmuir adsorption isotherm. Tafel plots indicate that both the compounds are mixed-type inhibitors and electrochemical analysis has similar results as obtained from gravimetric analysis. The SEM analysis agrees the surface protection of mild steel in presence of inhibitors.

## REFERENCES

- Abiola OK, Oforka NC, Adsorption of (4-amino-2-methyl-5-pyrimidinyl methylthio) acetic acid on mild steel from hydrochloric acid solution (HCl)—Part 1, *Materials Chemistry and Physics*, 83 (2-3), 2004, 315–322.
- Avci G, Inhibitor effect of N,N-methylenediacrylamide on corrosion behavior of mild steel in 0.5 M HCl, *Materials Chemistry and Physics*, 112 (1), 2008, 234–238.
- Bentiss F, Lebrini M, Lagrenee M, Thermodynamic characterization of metal dissolution and inhibitor adsorption processes in mild steel/2,5-bis(n-thienyl)-1,3,4-thiadiazoles/hydrochloric acid system, *Corrosion Science*, 47 (12), 2005, 2915–2931.
- Cao PG, Yao JL, Zheng JW, Gu RA, Tian ZQ, Comparative Study of Inhibition Effects of Benzotriazole for Metals in Neutral Solutions As Observed with Surface-Enhanced Raman Spectroscopy, *Langmuir*, 18 (1), 2002, 100–104.
- Dandia A, Gupta SL, Singh P, Quraishi MA, Ultrasound-Assisted Synthesis of Pyrazolo[3,4-b]pyridines as Potential Corrosion Inhibitors for Mild Steel in 1.0 M HCl, *ACS Sustainable Chemistry & Engineering*, 1 (10), 2013, 1303–1310.
- Ezeoke AU, Adeyemi OG, Akerele OA, Obi-Egbedi NO, Computational and experimental studies of 4 aminoantipyrine as corrosion inhibitor for mild steel in sulphuric acid solution, *International Journal of Electrochemical Science*, 7 (1), 2012, 534–553.
- Fragoza-Mar L, Olivares-Xometl O, Domínguez-Aguilar MA, Flores EA, Arellanes-Lozada P, Jimenez-Cruz F, Corrosion inhibitor activity of 1,3-diketone malonates for mild steel in aqueous hydrochloric acid solution, *Corrosion Science*, 61, 2012, 171–184.
- Gopal ji, Shukla SK, Dwivedi P, Sundaram S, Prakash R, Inhibitive effect of Argemone mexicana plant extract on acid corrosion of mild steel, *Industrial & Engineering Chemistry Research*, 50 (21), 2011, 11954–11959.
- Guan NM, Xueming L, Fei L, Synergistic inhibition between o-phenanthroline and chloride ion on cold rolled steel corrosion in phosphoric acid, *Materials Chemistry and Physics*, 86 (1), 2004, 59–68.
- Hong S, Liqin Y, Angela N, Vincenzo C, Yadong C, Lucia A, Qidong Y, Novel N-hydroxybenzamide-based HDAC inhibitors with branched CAP group, *Bioorganic & Medicinal Chemistry Letters*, 19 (22), 2009, 6284–6288.
- Hong T, Jepson WP, Corrosion inhibitor studies in large flow loop at high temperature and high pressure, *Corrosion Science*, 43 (10), 2001, 1839–1849.
- Jeeva M, Prabhu GV, Boobalan MS, Rajesh CM, Interactions and Inhibition Effect of Urea-Derived Mannich Bases on a Mild Steel Surface in HCl, *Journal of Physical Chemistry C*, 119 (38), 2015, 22025–22043.
- Kashyap SJ, Garg VK, Sharma PK, Kumar N, Dudhe R, Gupta JK, Thiazoles: having diverse biological activities, *Medicinal Chemistry Research*, 21 (8), 2012, 2123–2132.
- Kumar S, Sharma D, Yadav P, Yadav M, Experimental and Quantum Chemical Studies on Corrosion Inhibition Effect of Synthesized Organic Compounds on N80 Steel in Hydrochloric Acid, *Industrial & Engineering Chemistry Research*, 52 (39), 2013, 14019–14029.
- Li W, He Q, Zhang S, Pei B, Hou B, Some new triazole derivatives as inhibitors for mild steel corrosion in acidic medium, *Journal of Applied Electrochemistry* 38 (3), 2008, 289–295.
- Martinez S, Štagljar I, Correlation between the molecular structure and the corrosion inhibition efficiency of chestnut tannin in acidic solutions, *Journal of Molecular Structure: THEOCHEM*, 640 (1-3), 2003, 167–174.
- Moretti G, Quartarone G, Tassan A, Zingales A, Inhibition of mild steel corrosion in 1N sulphuric acid through indole, *Materials and Corrosion*, 45 (12), 1994, 641–647.
- Noor EA, Temperature Effects on the Corrosion Inhibition of Mild Steel in Acidic Solutions by Aqueous Extract of Fenugreek Leaves, *International Journal Electrochemical Science*, 2 (12), 2007, 996–1017.
- Oguzie EE, Njoku VO, Enenebeaku CK, Akalezi CO, Obi C, Effect of hexamethylpararosaniline chloride (crystal violet) on mild steel corrosion in acidic media, *Corrosion Science*, 50 (12), 2008, 3480–3486.



Ostovari A, Hoseinie SM, Peikari M, Shadizadeh SR, Hashemi SJ, Corrosion inhibition of mild steel in 1 M HCl solution by henna extract: a comparative study of the inhibition by henna and its constituents (lawsone, gallic acid, aD-glucose and tannic acid), Corrosion Science, 51 (9), 2009, 1935–1949.

Popova A, Sokolova E, Raicheva S, Chritov M, AC and DC study of the temperature effect on mild steel corrosion in acid media in presence of benzimidazole derivatives, Corrosion Science, 45 (1), 2003, 33-58.

Singh AK, Inhibition of Mild Steel Corrosion in Hydrochloric Acid Solution by 3-(4-((Z)-Indolin-3-ylideneamino)phenylimino)indolin-2-one, Industrial & Engineering Chemistry Research, 51 (8), 2012, 3215–3223.

Szklarska-Smialowska Z, Mankowski J, Crevice corrosion of stainless steels in sodium chloride solution, Corrosion Science, 18 (11), 1978, 953 - 960.

Szyprowski AJ, Relationship between chemical structure of imidazoline inhibitors and their effectiveness against hydrogen sulphide corrosion of steels, British Corrosion Journal, 35 (2), 2000, 155-160.

Xianghong Li, Deng S, Fu H, Taohong Li, Adsorption and inhibition effect of 6-benzylaminopurine on cold rolled steel in 1.0 M HCl, Electrochimica Acta, 54 (16), 2009, 4089–4098.

Yurt A, Ulutas S, Dat H, Electrochemical and theoretical investigation on the corrosion of aluminium in acidic solution containing some Schiff bases, Applied Surface Science, 253 (2), 2006, 919-925.

Zarrouk A, Hammouti B, Dafali A, Bentiss F, Inhibitive Properties and Adsorption of Purpald as a Corrosion Inhibitor for Copper in Nitric Acid Medium, Industrial & Engineering Chemistry Research, 52 (7), 2013, 2560–2568.

Zhao L, Teng HK, Yang YS, Tan X, Corrosion inhibition approach of oil production systems in offshore oilfields, Materials and Corrosion, 55 (9), 2004, 684–688.

Zou CJ, Yan XL, Qin YB, Wang M, Liu Y, Inhibiting evaluation of  $\beta$ -Cyclodextrin-modified acrylamide polymer on alloy steel in sulfuric solution, Corrosion Science, 85, 2014, 445–454.